JOURNAL GEOLOGICAL SOCIETY OF INDIA
Vol.88, July 2016, pp.29-38

Mapping Lithology and Assessing Recharge Characteristics in a Granitic Hard Rock Aquifer: Inference from 2D Resistivity, Induced Polarization, Tracer and Moisture Measurements

Dewashish Kumar[1]*, G.B.K Shankar[1], Setbandhu Mondal[1], V. Venkatesam[1], K. Sridhar[1], P. N Rao[2], Pandith Madhnure[2] and R. Rangarajan[1]

[1]CSIR-National Geophysical Research Institute, Hyderabad – 500007
[2]Central Ground Water Board, Southern Region, Hyderabad
***Email:** dewashishkumar@ngri.res.in

Abstract: Two dimensional Electrical Resistivity Tomography (ERT) investigation along with Time Domain Induced Polarization (TDIP) investigation covering 1.6 km line were carried out at 3 natural recharge sites in a overexploited groundwater granite watershed, situated in a semi arid region in the state of Telangana, India. At these sites, shallow and/or deep moisture influx measurements were also carried out using injected tritium tracer and neutron moisture probe. The watershed is covered by sandy loam to silt loam soil, receives an average annual rainfall of 620 mm with the pre monsoon groundwater level ranging from 8m to 29m bgl. The spot investigations were done to assess and understand the recharge process and groundwater potential in terms of resistivity/conductivity and moisture characteristics of the subsurface rock formation.

The measured and 2D inverted resistivity models shows soil, highly weathered and moderately weathered zones up to a depth of 22m followed by semi-weathered and massive granites up to the maximum depth of 78m. The resistivity values of the soil and shallow weathered zones varying between ~5-50 Ohm.m up to a depth of 12m. The large variation in resistivity values of the soil and weathered zone is probably indicative of large variation in the moisture potential. The resistivity models clearly mapped the granitic hard rock structure in the depth range of 22 – 78m, which has a significant resistivity contrast (~1500-11000 Ohm.m) with respect to the overlying semi weathered layers. The modeled 2D resistivity data at a site in two perpendicular directions shows similar geological structure and geoelectric layers. The TDIP dataset shows insignificant chargeability variations (1-7 mV/V) up to the investigated depth of 78m, which probably indicates low to moderate moisture and groundwater potential in the vadoze and saturated zones of the aquifer. The experimental investigations provide scope for assessing dynamic recharge and groundwater potential at selected sites in an overexploited granite watershed in the present geological context.

Keywords: ERT and TDIP investigations, granitic terrain, recharge, aquifer potential

INTRODUCTION

The dependence of groundwater for domestic, industrial and irrigation sectors has increased several folds in last few decades. The exploitation of groundwater is predominant in hard rock areas of India. The trend of increase in groundwater exploitation for domestic and agricultural sectors is likely to continue forever where surface water resources are not available. The over-exploitation of groundwater resources has resulted in water level decline and quality deterioration in large parts of semi arid regions.

Recharge is a vital parameter to be known for groundwater budgeting, management and modeling studies. The study of recharge to the hard rock aquifer system is an important thrust area to understand, evaluate and estimate dynamic groundwater potential for sustainable management of groundwater resources in the hard rock aquifer system. The knowledge of sub-surface lithology, strata and their characteristics is prerequisite in the groundwater recharge studies. Groundwater recharge is a function of the annual average rainfall, hydrological characteristics, geology of the area, slopes and nature of the soil. Increase in rainfall leads to increase in the groundwater level. Conversely decrease in rainfall leads to groundwater depletion (Igboekwe and Adindu, 2011). The groundwater level in a fractured rock aquifer responds quickly to rainfall although the bedrock was covered by 10m thick till soil. The hypothesis that the bedrock aquifer was recharged by

vertical flow from groundwater in the overlying soil was tested with a simple recharge model, in which the bedrock groundwater levels were simulated from the soil groundwater and estimated surface loading variation. The model has three parameters. The ratio between the equivalent vertical hydraulic conductivity governing the recharge and the storage coefficient of the bedrock reservoir, the recession coefficient for the bedrock groundwater level and the bedrock groundwater level at which the outflow ceases. The model could be reasonably well calibrated and validated to head observations in one of two boreholes. The fit to the seasonal variation was similar when calibrating the model with or without surface loading but surface loading has to be included to properly simulate individual recharge events (Rodhe and Bockard, 2006). Artificial groundwater recharge is the process by which water from above surface is added to the saturated zone of an aquifer either directly or indirectly. Due to over exploitation of groundwater there is a decrease in the level of groundwater so that it cause increase level of saline water in coastal areas. Recharge shafts, injection wells, induced recharge, improved land and watershed management are employed to understand the system. Soil infiltration studies of area and chemical quality of water are the basic purpose of artificial groundwater recharge to restore supplies from aquifers depleted due to excessive groundwater development (Yadav et al., 2012). Similarly, in geophysics Electrical Resistivity Tomography (ERT) and Self Potential (SP) technique was applied to find suitable locations for new water wells in the zones with little hydrogeological data but it need large fractured zones for the drillings. Long ERT profiles allowed us to image the resistivity distribution of the deeper sub-surface structure of the geological strata and to detect and characterize the fractured zone(s), which is expected to be less resistive compared to the massive rock. On the other hand, SP measurements have negative anomalies possibly related to preferential flow pathways. Apparent coupling coefficient between SP signals and differences in hydraulic heads are also estimated in order to image the water table (Robert et al., 2011). In recent study Gazoty et al. (2012) has carried out a direct current (DC) resistivity and time domain induced polarization (TDIP) investigation for mapping the waste deposits and to discriminate important geological units that control the hydrology. TDIP has nicely delineated clay making the TDIP technique possible to enhance the resolution of geological structures compared to DC surveys alone (Gazoty et al., 2012). Low frequency geoelectrical methods include mainly self potential, resistivity, and induced polarization techniques, which have potential in many environmental and hydrogeological applications. Electrical resistivity parameter is dependent on the water content, the temperature, the salinity of the pore water, clay content and the mineralogy. Induced polarization characterizes the ability of rocks to reversibly store electrical energy (Revil et al., 2012). In an important study in different type of hard rock settings Kumar (2012) has studied the efficacy of the electrical tomography technique in mapping the bedrock depth and basement topography, dyke characteristics, deeper groundwater resources and fault zones related to groundwater hydrogeology. In another study Kumar et al., (2011) delineated the fault zones and mapped the geothermal resources in Deccan Trap region employing high resolution electrical resistivity tomography. This study clearly brings out the characteristics of the conducting mineralization fluid and the normal fluid based on the substantial resistivity contrast as seen from the model resistivity dataset (Kumar et al., 2011). Kumar et al. (2014) studied 2D inverted resistivity model dataset and it shows clear cut soil moisture unsaturated zone up to a depth of 22m. This zone revealed quite a large variation in the moisture content within the weathered granitic layers, which holds the moisture within the pores spaces of the rock matrix.

STUDY AREA

Madharam watershed in Midjil Mandal, Mahabubnagar district in the state of Telangana, India lies between latitudes $16^0$37'46" N to $16^0$47'41" N and longitudes $78^0$21'16" E to $78^0$26'02" E (Fig.1a). The watershed covers an area of 95 km^2 is located in granitic terrain and it receives an average annual rainfall of 620mm. Moderately weathered pediplain and shallow weathered pediplain occupy major part of the watershed area. The experimental recharge sites are located in moderately weathered pediplain (Table 1). The watershed area is mostly covered by sandy loam to silt loam soils with a maximum depth of 2.5m. The watershed slopes from north to south and the topographic elevation varies from 560m amsl in the north to 460m amsl near Dindi river in the south. The area has two major irrigation tanks, 9 minor irrigation tanks and water conservation

Table 1. Shows the experimental recharge sites signifying surface condition, hydrogeological condition, depth of weathering and the nature of soil at three sites.

Site no.	Site name	Surface condition	Depth of weathering (m)	Static water level in observation well (m bgl)	Surface soil type
1.	Madharam school	Rainfed land	15.3	18-20	Sandy loam
2.	Urukonda	Paddy field	39.2	15-17.5	Silty
3.	Near Madharam	Paddy field	11.0	18-20	Silty

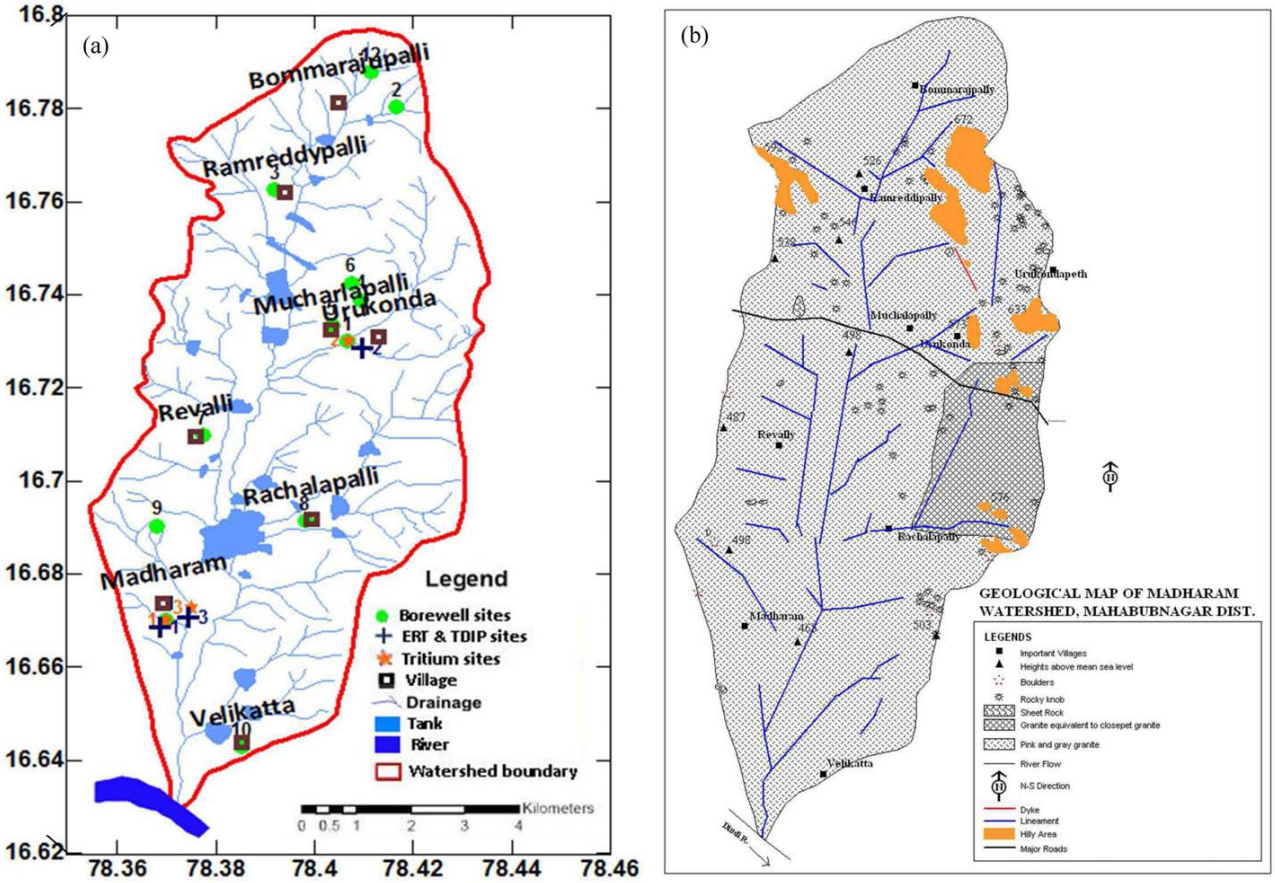

Fig.1. Shows the Madharam watershed with detailed features **(a)** Depicts the borewell location, village names, drainage pattern, tank, river, ERT & TDIP sites and tritium (recharge) sites. **(b)** Shows the detailed geological map with major rock unit, geological structure in Madharam watershed, Mahabubnagar district Telangana.

structures like percolation tanks and check dams. The area is totally dependent on groundwater excluding some parts below the existing major tanks for all drinking and irrigation purposes and is categorized as over exploited basin as on 2004 (stage of ground water development is 129%, CGWB (2007)).

GEOLOGY AND HYDROGEOLOGY

The watershed is underlain by pink and grey granites of Archaean age. A dolerite dyke/intrusion trending in NNW-SSE direction is observed in eastern part of the study area (Fig.1b). Three sets of lineaments trending NNW-SSE, NE-SW and NNE-SSW are observed in the area. The pink granite is massive, occasionally gneissic and intrusive into the Dharwar schist and grey gneisses. The grey granite is banded, the light bands being rich in quartz and feldspar and the dark bands rich in mica and hornblende. Groundwater occurs under semi-confined to confined conditions in the present geological setting. Groundwater is exploited through borewells of depth ranging from 30 to 60m below ground level (bgl) and their discharge ranges from 1 to 5 liter/second (lps). The depth to water levels varies from 8m to 29m bgl during pre-monsoon and 7.8m to 19.94 m bgl during post-monsoon.

MATERIALS AND METHODS

2D Electrical Resistivity Tomography and Time Domain Induced Polarization

Two dimensional Electrical Resistivity Tomography (ERT) along with Time Domain Induced Polarization (TDIP) dataset with 8 windows timing set up and equal duration for current-on and current-off in the measurement cycle were acquired at 3 selected natural recharge sites covering 1.6 km line (Fig.1a) and deployed gradient as well as dipole-dipole array for complete set of data acquisition. The dipole-dipole array provided high resolution shallower depth information for detailed sub-surface lithology. At the same time, the gradient array has advantage in faster data

acquisition with better signal to noise ratio in resolving geological structure (Loke, 2004). The full waveform resistivity and TDIP dataset offers a flexibility of monitoring of output current and voltage with full waveform sampling and recording of the dataset (ABEM, 2012). In TDIP measurement, the integration of time is calculated for each time window, which is a multiple of the time period of 20 ms in order to suppress power line noise so as to achieve actual signal from the subsurface rock strata. At one site, two sets of 2D ERT profiles completed in perpendicular direction to analyze the moisture variation within the subsurface geoelectric layers in orthogonal directions. The 2D measured apparent resistivity and chargeability dataset were first analyzed and later processed for eliminating any noisy or bad data points in the gathered dataset. The apparent field dataset do contain anomalies of the subsurface body as is clearly reflected and viewed from the 2D pseudosections at different sites. The field datasets are presented in the form of pseudosections with dense sampling of apparent resistivity and apparent chargeability measurements at shallow depth (Loke, 1997, 2012) with vast coverage both in lateral and vertical directions. The processed and filtered dataset is inverted using least squares inverse approach with smoothness constrained (Sasaki, 1992; Loke, 1997, Loke et al., 2010 and Loke, 2012) and with a standard Gauss-Newton optimization technique by the help of recent version of Res2DINV. This actually reproduces a realistic sub-surface 2D inverted resistivity and chargeability models with depth both in the lateral and vertical directions. These 2D inverted models of the sub-surface geology presented in the form of resistivity and chargeability revealed the sub-surface geological layers, structures, hydrogeological features based on the resistivity and chargeability contrasts with respect to the host rock. These 2D inverted resistivity and chargeability models represent the sub-surface realistic picture and ultimately interpreted in terms of different rock layers, lithology and structure (Kumar, 2012) for groundwater studies.

Shallow moisture flux and depth moisture measurements

The tritium injection method based on piston flow model for the movement of water infiltrating the vadoze zone (Zimmermann *et al.*, 1967, Munnich *et al.*, 1967, Munnich, 1968) is used for shallow moisture influx measurements at the selected recharge sites. In the tritium injection method, the moisture at a certain depth (60-80cm) in the soil is artificially tagged with tritiated water. For estimating rainfall recharge or irrigation return flow flux, the injections are made before the onset of monsoon/sowing of crop. The tracer moves downwards due to infiltration of a fraction of precipitation or irrigation water within a soil profile. A soil core is collected from the injection site after the monsoon or at the end of one hydrological cycle and the moisture content and tracer concentration is measured in samples from successive depth intervals. The displaced position of the tracer is indicated by the peak in its concentration in a plot of depth versus tritium activity. The moisture content of the soil column between the injection depth and displaced depth of the tracer in the soil core is the measure of recharge to groundwater over the time interval between injection of tritium and collection of soil core. The laboratory and field investigations for measurement of recharge at a given site are described in detail by Rangarajan and Athavale (2000). Tritium tracer of 15 micro curie/liter was injected below 60cm depth before the onset of monsoon at the selected 3 recharge (tritium) sites namely 1, 2 and 3 (Fig.1a). Vertical soil samples of 20cm interval (depth wise) are collected using recovery pipes up to a depth of 2m after post-monsoon season. The depth samples were analyzed in the laboratory for moisture content through gravimetric method and tracer concentration using liquid scintillation counter. Depth wise tritium and moisture data at each site was used for evaluating moisture flux at each site. The moisture influx or the amount of water added per square millimeter of the soil below the root zone, was calculated by determining the peak of tritium profile and the moisture content of the zone between the injection depth and depth of the displaced tritium spiked layer and is given by equation 1.

$$\mathrm{Re} = \left[\frac{m_d}{(100 + m_d)} \right] \gamma_w h. \qquad (1)$$

where, Re= Recharge; m_d =dry weight percent of soil moisture; γ_w = wet-bulk density of the soil in situ; h = displacement of tracer, i.e. the distance between injection depth and the centre of gravity of the profile.

The neutron technique for soil moisture measurement is based on the effective slowing down of fast neutrons by the hydrogen present in water compared to other elements present in the soil matrix. The slow neutron density around the fast neutron source when kept in moist soil, varies according to moisture content i.e. hydrogen concentration of the soil. This slow neutron density is measured and correlated to the moisture content of the soil. The neutron moisture probe consists of a fast neutron source near a slow neutron detector with associated electronic circuitry. The neutron Amercium 241 – Berilium source is used in the neutron moisture probe. The fast neutrons emitted are thermalized or slowed by the hydrogen (water) in the material. The ideal detector which can be used with moisture

gauge should have high efficiency for slow neutrons and should be insensitive to fast neutrons and gamma radiations. In the present gauge Helium-4 detector is used.

Depth moisture measurements up to maximum depth of 12m were observed at two of the three recharge sites, one each in rainfed and irrigated land. For the measurement of moisture content with depth probe, an access tube (aluminum) is inserted in the soil with bottom closed to avoid entry of moisture in the tube. The soil moisture probe is inserted into the access tube at varying depths. The response of the probe in the soil is noted. From this response the moisture content of the soil at the measurement position is obtained from the calibration graph. The moisture content of the soil thus indicated depends upon many field parameters as well as on the accuracy of the calibration and precision in the measurement.

RESULTS

The 2D inverted resistivity models at the natural recharge sites (sites 1, 2 and 3) shows layered earth structure with distinct layers both in the gradient and dipole –dipole arrays dataset (Fig.2). The near surface layer in the models shows low resistivity ~25-50 Ohm.m at site 1 (Fig. 2a), ~15-50 Ohm.m at site 2 (Fig. 2b) and less than 10 Ohm.m at site 3 (Fig. 2c) indicating highly weathered granite formations up to a depth of 12m. This layer is followed by resistivity values of 100-700 Ohm.m at site 1, 110-1110 at site 2 and ~50-400 Ohm.m at site 3 indicating semi-weathered granite formations, which extends down to a maximum depth of 40m. Further downward, there is a gradual increase in resistivity from 40m to a depth of 78m (the maximum depth of investigation) at all the three sites (Fig.2), which indicates the basement granitic rock. The maximum model resistivity values resolved at the bottom depth are ~11000 Ohm.m at site 1, ~4000 at site 2 and ~8000 Ohm.m at site 3 (Table 2), which represents the fresh massive granite with no fracturing and fissuring. The perpendicular 2D resistivity profile laid at site 3, reveals similar value of the resistivity range for weathered and massive granite all along the profile. The 2D chargeability sub-surface models at all the three recharge sites shows a uniform variation of chargeability values. It is in the range of 3-5 mV/V at site 1, 1-7 mV/V at site 2 and 1-3 mV/V at site 3, all along the sub-surface in x and z dimensions (Fig.3). The interpreted and inferred results of resistivity and chargeability variation for three major layers

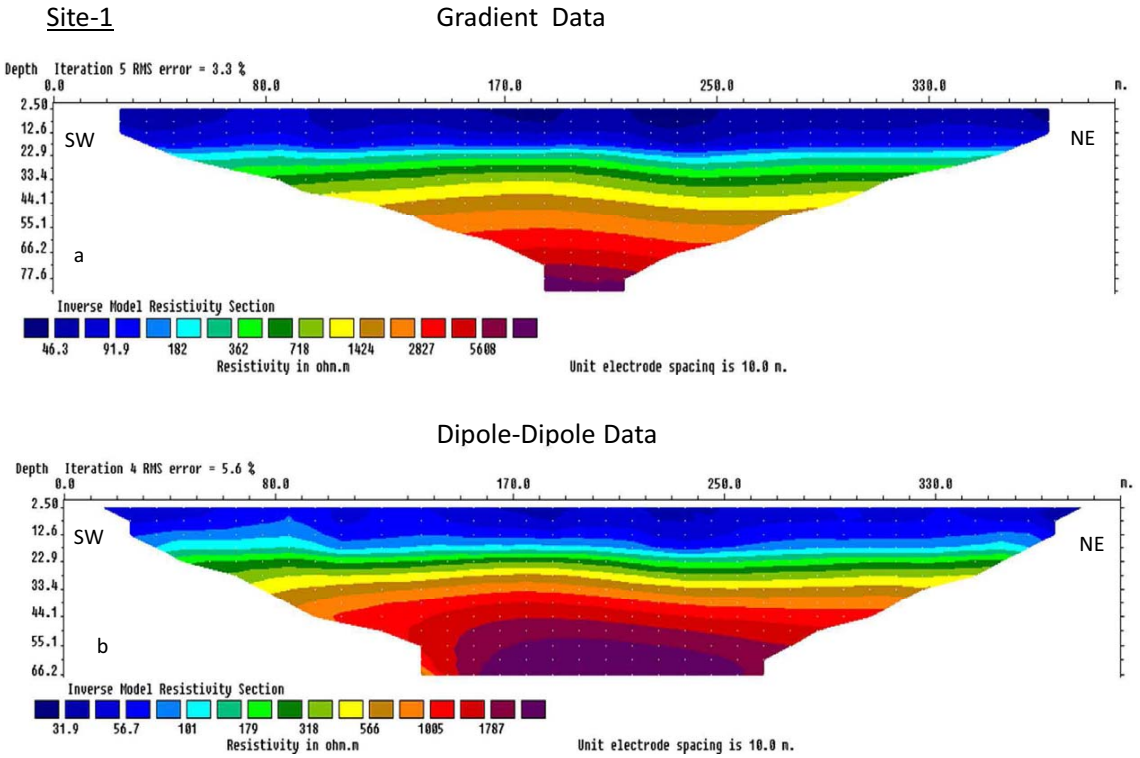

Fig.2. Shows the gradient and dipole-dipole 2D inverted resistivity models with substantial resistivity contrast between the shallow and the deeper layers at the three recharge sites (site 1: rainfed, sites 2, 3 irrigated area). At all the three sites the models clearly revealed the low resistivity (~10-50 Ohm.m) at the near surface layers while the massive basement granitic rock (1500 – 11000 Ohm.m) at the deeper depth levels.

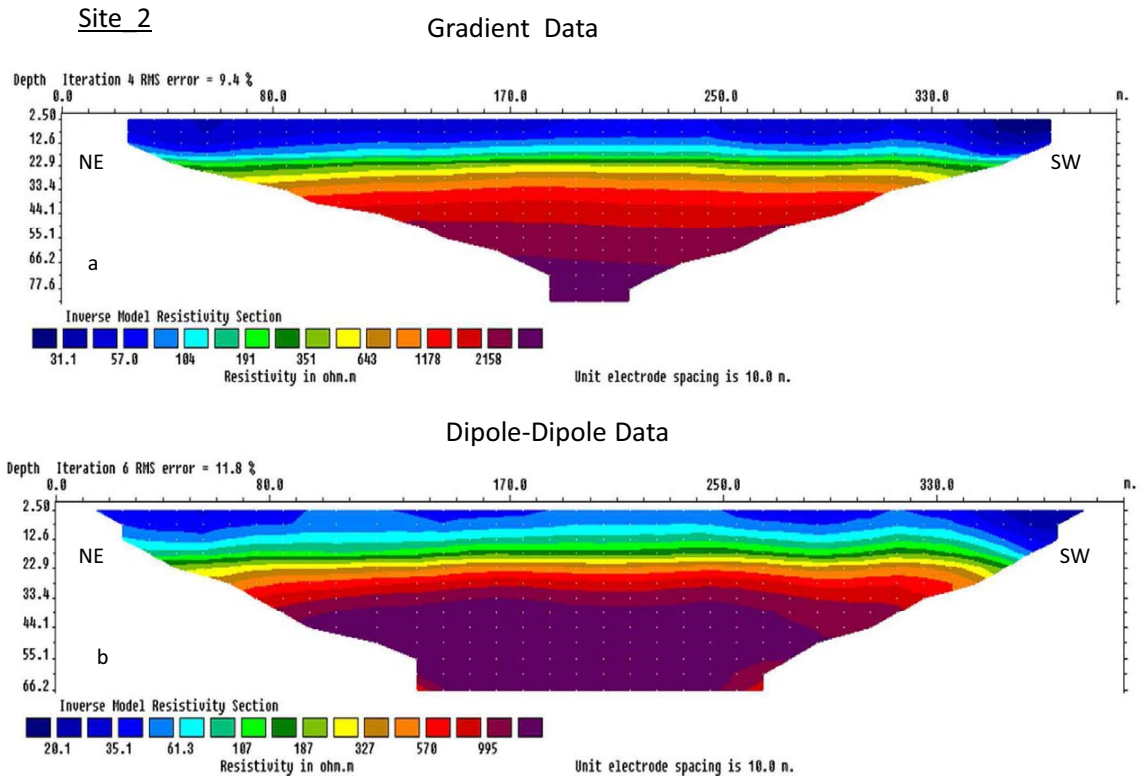

Fig. 2b Shows the gradient and dipole-dipole 2D inverted resistivity models with substantial resistivity contrast between the shallow and the deeper layers at site 2, Urukonda.

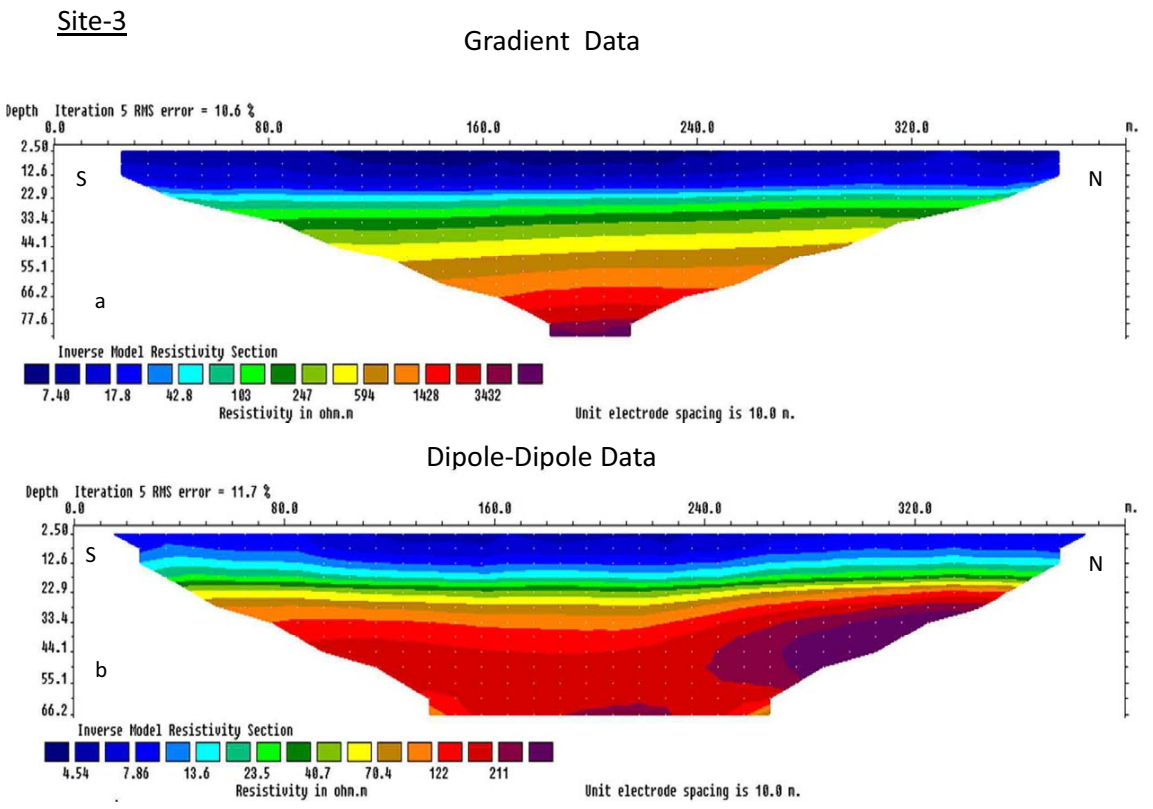

Fig.2c. Shows the gradient and dipole-dipole 2D inverted resistivity models with substantial resistivity contrast between the shallow and the deeper layers at site 3, near Madharam.

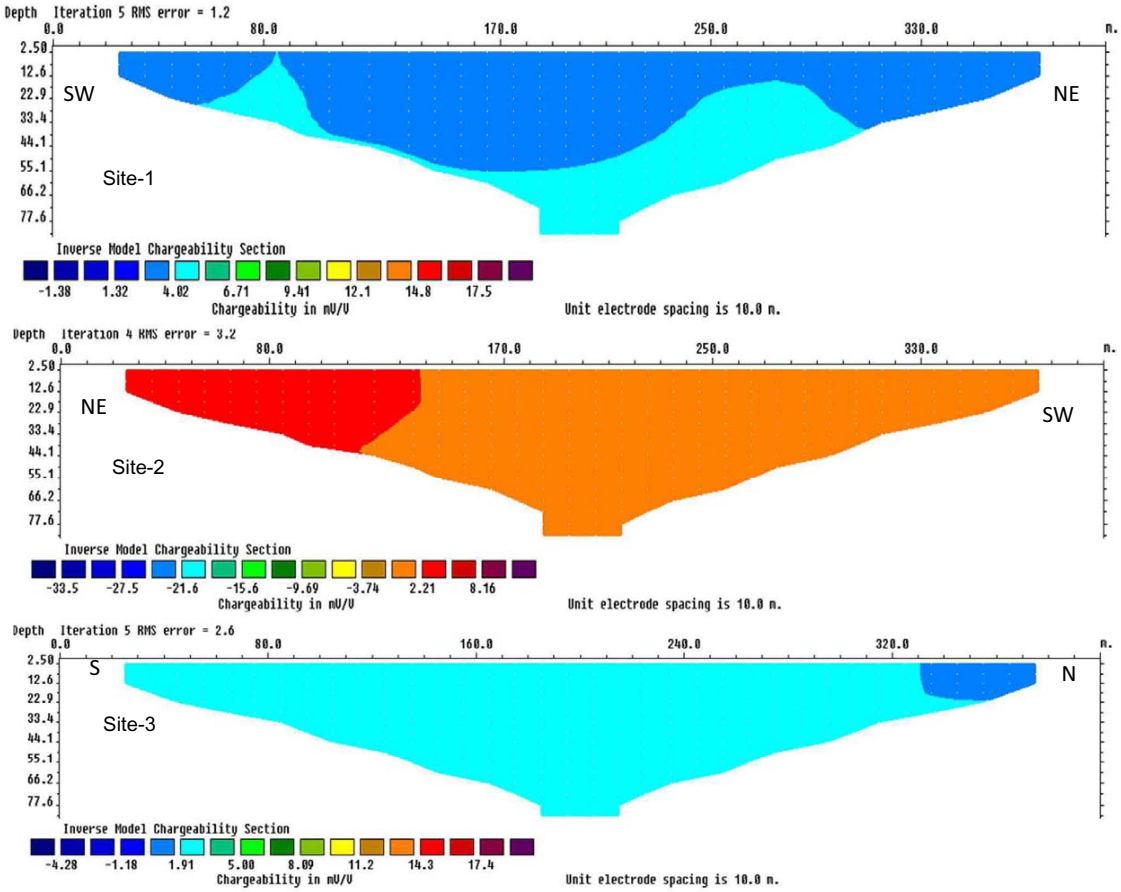

Fig.3. Shows the time domain induced polarization (TDIP) 2D inverted chargeability models at the recharge sites showing gentle variation of chargeability values at all the 3 sites.

namely weathered, semi-weathered with fracture and massive granite at the individual site is given in Table 2. The shallow moisture influx measurements based on tritium peak migration caused by rainfall and depth moisture measurements at the rainfed site (site 1) is shown in Fig.4. The recharge estimated at this rainfed site is only 21.2 mm, which is equivalent to 3.2% of the effective rainfall of 647 mm. The average volume moisture variation at this site is 17-20 % within the shallow zone of 150cm and reduces to 12-17% at deeper zone up to the depth of 10m with the change in moisture flux as 1.8%. Shallow moisture influx measurements based on tritium peak migration caused by rainfall and irrigation and depth moisture measurement at paddy field site (site 3, irrigated site) is shown in Fig.5. The recharge rate estimated is 226 mm at site 2 and 206 mm at site 3 for the combined input amount of rainfall and irrigation. The average increase in moisture flux calculated due to rainfall and irrigation during the period of August to September, 2010 is 4% up to the depth of 4.5m. However, in the case of the irrigated field the moisture measurement during monsoon period is restricted to 5m only due to the significant rise of water level.

Table 2. Shows the classification of resistivity and chargeability and its characterization in to subsurface geoelectric layers based on the model parameters result at recharge sites

Recharge site no.	Model Parameters	Weathered granite	Semi-weathered granite	Massive granite
1.	Resistivity (Ohm.m)	25-50	100-700	~2000-11000
	Chargeability (mV/V)	3-4	4-5	5
2.	Resistivity (Ohm.m)	50-110	110-1110	~2000-4000
	Chargeability (mV/V)	1-7	3-5	2-3
3.	Resistivity (Ohm.m)	<10	50-400	~1500-8000
	Chargeability (mV/V)	1-3	2-3	2-3

DISCUSSION

The results of the high resolution 2D resistivity tomography at the three natural recharge sites in the granitic watershed reveals a layered lithological structure with substantial resistivity contrast between the shallow and deeper depth levels where the resistivity values are increasing with depth. This interpretation is well supported by the borehole drilled near the site no.2 at Urukonda. The

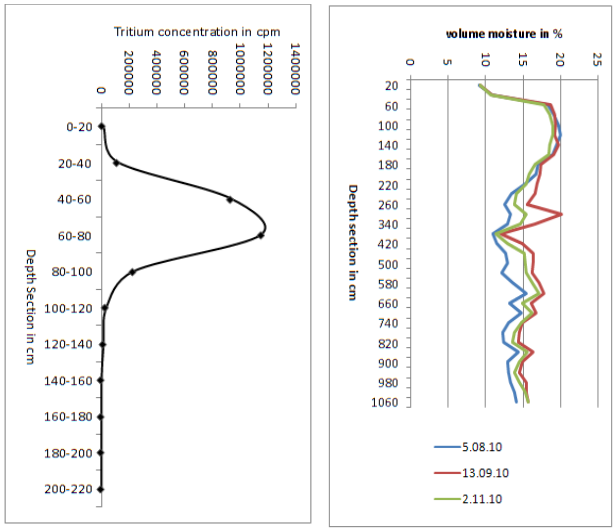

Fig.4. Shows the tritium and depth moisture profiles at a rainfed site (site 1) and the relation with moisture content where the tritium concentration in counts/minute (cpm) and volume moisture in % at Madharam watershed.

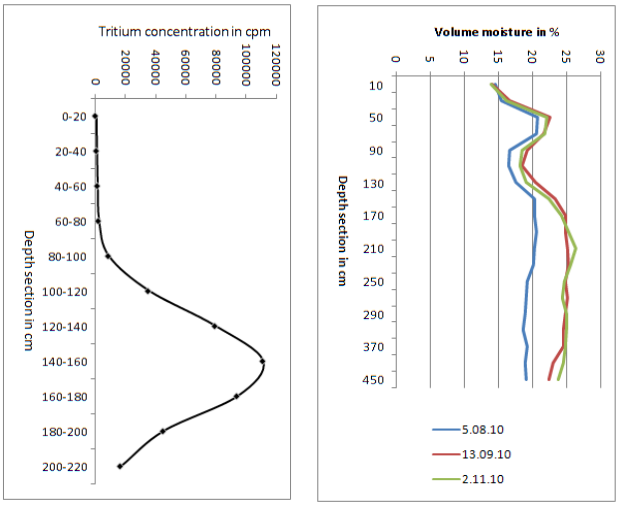

Fig.5. Shows the tritium and depth moisture profiles at an irrigated site (site 3) and the relation with moisture content where the tritium concentration in counts/minute (cpm) and volume moisture in % at Madharam watershed.

litholog and electrical log are shown in Fig.6 and Fig.7 (CGWB unpublished report) respectively. This litholog is well corroborated with the 2D inverted resistivity model in terms of resistivity. A comparison between the electrical resistivity log and electrical resistivity tomography is made in order to classify the lithological formations right from the near surface layer to a depth of 65m as presented in Table 3 and helped in establishing the litho-resistivity relationship. The resistivity values obtained from the log responses (Fig.7) are in good agreement with the modeled values of resistivity from the electrical tomography study

Table 3. Comparison between resistivity values obtained through electrical resistivity logging and Electrical Resistivity Tomography (ERT) result at different depth levels at Urukonda, site no.2

Formation	Depth (m)	Resistivity in Ohm.m (through electrical logging) 16" Normal	64" Normal	(through ERT imaging survey)
Soil and highly weathered granite	0-12	—	—	15-50
Weathered granite	12-23	—	—	50-110
Semi-weathered granite, fracture zone	23-38	250-800	700-1000	110-1110
Massive granite, fracture zone	38-65	2000-2600	6700-7500	1200-3950

(Fig.2b). The detailed description is shown in Table 3. The near surface lower resistivity values at all the three sites in the range of <10-50 Ohm m suggest that the infiltration capacity and percolation rates are good as indicated by higher shallow moisture influx rates observed by tritium profiles at the irrigated sites (site 2 and 3) and significant (4%) increase in moisture influx rate at neutron moisture measurement irrigated site up to a depth of 4.5m. It is expected that the moisture potential in the shallow zone up to a depth of few meters below ground level will be higher at the irrigated sites in comparison to the rainfed sites where the water input is due to rainfall alone. Thus the higher moisture potential due to irrigation in the near surface layers drops the resistivity value to <10 Ohm.m as inferred from the resistivity models in comparison to the resistivity values

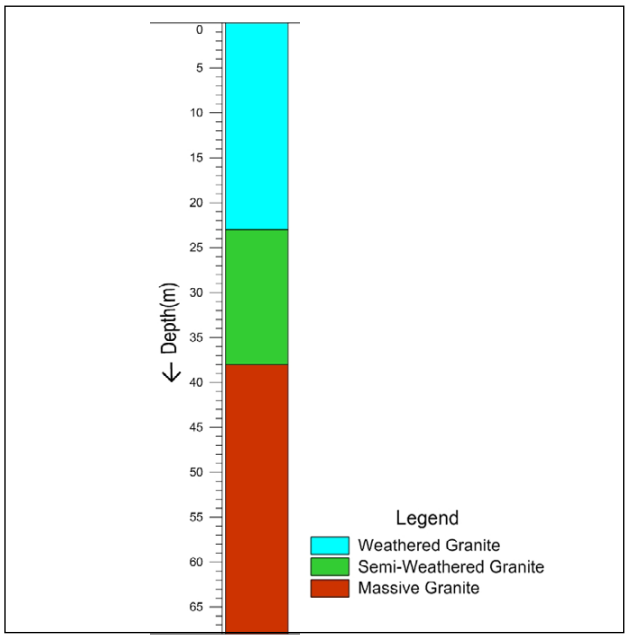

Fig.6. Shows the borehole litholog for the drilled well near the ERT site no.2 at Urukonda, which show the major three layers viz., weathered, semi-weathered and massive granite.

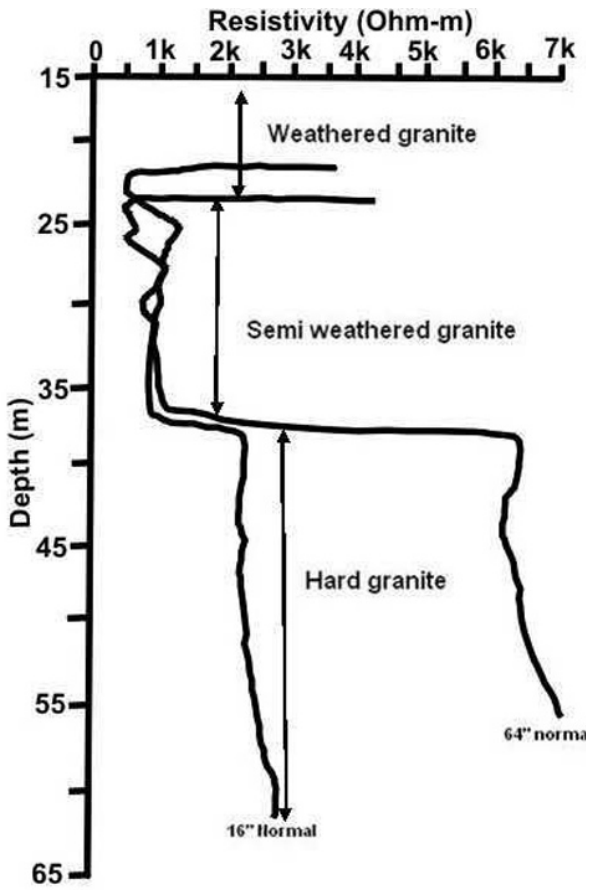

Fig.7. Shows the electrical log and its interpretation for the exploratory well-1 constructed at Urukonda, Mahabubnagar district, Telangana (Location: 16°43'38"N, 78°24'24"E) close to the electrical resistivity tomography site no.2.

(25-50 Ohm.m) of the shallow zone at the rainfed site (site 1).

The weathered layer and the massive granite are well mapped, while the semi-weathered/fractured granitic layer sandwiched between the weathered and massive layers is quite visible with a resistivity contrast between ~100-600 Ohm.m. In these zones, the possibility of minor or sparse fracture could exist, which acts as aquifer and is a source of groundwater. This is supported by change in water level of 2.9m of the semi-confined aquifer zones observed during active monsoon period. The chargeability values ~1-7 mV/V modeled from time domain induced polarization dataset up to the maximum investigated depth of 78m at the recharge sites can be considered as low to moderate, which probably implies poor moisture and groundwater potential at the investigated sites.

CONCLUSIONS

The high resolution electrical resistivity tomography results are found to be useful in delineating soil/ highly weathered, moderately weathered zones and deeper massive granites and is well correlated with the drilled litholog data. The resistivity contrast is significant between the near surface lithological layers and the deeper massive granites. The model resistivity value of the order of ~10-50 Ohm.m as revealed up to the depth of 12m at the recharge sites suggests higher infiltration and percolation capacity of the near surface layers. The tritium and depth moisture data of shallow zone corroborated with the resistivity tomography dataset. The 2D inverted models show increase in resistivity values in the zone of 22-78 m depths. In the present study the characteristics resistivity range for the major granitic formations is established based on the drilled lithologs, electrical logging and the electrical tomography study. Nevertheless the substantial resistivity contrast and a uniform increase in resistivity with depth can be attributed to minor fracture zones in the present hard rock aquifer system. The inverted models show that the massive granite formation at a deeper depth has a resistivity value of the order of ~1500-11000 Ohm.m, indicating absence of any major fissures and fractures zone while the time domain induced polarization results indicates low magnitude chargeability values ~1-7 mV/V, which probably indicates poor to moderate moisture and groundwater potential at the investigated sites.

Acknowledgements: Authors are grateful to the former Director Prof. Mrinal K. Sen and the present Director, National Geophysical Research Institute, Hyderabad India for their kind permission and encouragement for carrying out the research work under inhouse MLP project. The financial assistance has been supported by grant from the MLP project is duly acknowledged here. The authors gratefully acknowledge an anonymous reviewer for his constructive comments, which improved the presentation.

References

ABEM (2012) ABEM Instruction manual: Terrameter LS Toolbox, 31p.

CGWB (2007) Groundwater information in Mahabubnagar district, Andhra Pradesh Southern region, Hyderabad Ministry of water resources July, 2007.

CGWB (unpublished report, 2011) - Geophysical Well logging in Mahabubnagar district, Andhra Pradesh by Narayana Raju, 2011.

Gazoty, A., Fiandaca, G., Pedersen, J., Auken, E., Christiansen, A.V. and Pedersen, J.K. (2012) Application of time domain

induced polarization to the mapping of lithotypes in a landfill site. Hydrology and Earth System Sci., v.16, pp.1793–1804.

Igboekwe, M.U. and Adindu, R. (2011) Groundwater Recharge through Infiltration Process A Case Study of Umudike, Southeastern Nigeria. Jour. Water Resource and Protection, v.3, pp.295-299.

Kumar, D. (2012) Efficacy of Electrical Resistivity Tomography technique in Mapping Shallow Subsurface Anomaly. Jour. Geol. Soc. India, v.80(3), pp.304-307.

Kumar, D., Thiagarajan, S. and Rai, S.N. (2011) Deciphering geothermal resources in Deccan Trap region using Electrical Resistivity Tomography Technique. Jour. Geol. Soc. India, v.78(6), pp.541-548.

Kumar, D., Shankar, GBK, Mondal, S., Venkatesam, V., Sridhar, K. and Rangarajan, R. (2014) Evaluating the recharge process and mapping lithology in granitic hard rock aquifer from full waveform 2D resistivity and IP dataset, published in abstract volume of 50th Annual Convention on "Sustainability of Earth System -The Future Challenges" held during 8-12 January, 2014 on the occasion of 'Golden Jubilee Celebrations' at CSIR-NGRI, Hyderabad, pp.187.

Loke, M.H. (1997) Electrical imaging surveys for environmental and engineering studies: A practical guide to 2-D and 3-D surveys, 61p.

Loke, M.H. (2004) Tutorial 2-D and 3-D electrical imaging surveys, pp.1-128.

Loke, M.H. (2012) 2D and 3D Resistivity/IP inversion and forward modeling, Geotomo Software Penang, Malaysia.

Loke, M.H., Wilkinson, P.B. and Chambers, J.E. (2010) Parallel computation of optimized arrays for 2-D electrical imaging surveys. Geophys. Jour. Internat., v.183, pp.1302-1315.

Munnich, K.O., Roether, W. and Thilo, L. (1967) Dating of groundwater with tritium and C-14, Isotope Hydrology, IAEA, Vienna, pp.305-320.

Munnich, K.O. (1968) Moisture movement measurement by Isotope tagging, *In:* Guide book on Nuclear techniques in Hydrology, IAEA, pp.112-117.

Rangarajan, R. and Athavale, R.N. (2000) Annual replenishable Ground water potential of India – An estimate based on injected tritium studies. Jour. Hydrology, v.234, pp.38-53.

Revil, A., Karaoulis, M., Johnson, T. and Kemna, A. (2012) Some low-frequency electrical methods for subsurface characterization and monitoring in hydrogeology, Hydrogeology Jour., v.20, pp.617–658.

Robert, T., Dassargues, A., Brouyere, S., Kaufmann, O., Hallet, V. and Nguyen, F. (2011) Assessing the contribution of electrical resistivity tomography (ERT) and self-potential (SP) methods for a water well drilling program in fractured/ karstified limestones. Jour. Appld. Geophys., no.75, pp.42-53.

Rodhe, A. and Bockard, N. (2006) Groundwater recharge in a hard rock aquifer A conceptual model including surface-loading effects. Jour. Hydrology, pp.389-401.

Sasaki, Y. (1992) Resolution of resistivity tomography inferred from numerical simulation, Geophys Prospect., v.40, pp.453–464.

Yadav, A., Sonje, A., Mathur, P. and Jain, D. A. (2012) A review on Artificial groundwater recharge. Internat. Jour. Pharma and Bio Sci., v.3(3), pp.304-311.

Zimmermann, U., Munnich, K.O. and Roether, W. (1967) Downward movement of soil moisture traced by means of Hydrogen Isotopes, Geophysical Monograph.

(Received: 14 October 2014; Revised form accepted: 13 July 2015)